The Journal of Neuroscience, October 15, 1998, *18*(20):8133–8144

Postsynaptic Mechanisms Underlying Responsiveness of Amygdaloid Neurons to Nociceptin/Orphanin FQ

Susanne Meis and Hans-Christian Pape

Institut für Physiologie, Otto-von-Guericke-Universität, D-39120 Magdeburg, Germany

Effects of nociceptin/orphanin FQ (N/OFQ), the endogenous ligand of the opioid-like orphan receptor (ORL), were investigated in the rat lateral (AL) and central (ACe) amygdala *in vitro*. Approximately 98% of presumed projection neurons in the AL responded to N/OFQ with an increase in inwardly rectifying potassium conductance, resulting in an impairment in cell excitability. Half-maximal effects were obtained at 30.6 nM; the Hill coefficient was 0.63. In the ACe, 31% of the cells displayed responses similar to that in the AL, 44% were nonresponsive, and 25% responded with a small potassium current with a linear current–voltage relationship. Responses to N/OFQ were reduced by 100 μM Ba^{2+}, were insensitive to 10 μM naloxone, and were blocked by a selective ORL antagonist, [$Phe^1\psi(CH_2$-$NH)Gly^2$]$NC(1–13)NH_2$ (IC_{50} = 760 nM). Involvement of G-proteins was indicated by irreversible effects and blockade of action of N/OFQ during intracellular presence of GTP-γ-S (100 μM) and GDP-β-S (2 mM), respectively, and prevention of responses after incubation in pertussis toxin (500 ng/ml). These mechanisms may contribute to the role of N/OFQ in the reduction of fear responsiveness and stress that have recently been suggested on the basis of histochemical and behavioral studies.

Key words: nociceptin; orphanin FQ; amygdala; electrophysiology; pharmacology; potassium inward rectifier

A heptadecapeptide, termed nociceptin (Meunier et al., 1995) or orphanin FQ (Reinscheid et al., 1995), has recently been identified as the endogenous agonist for an opioid receptor-like protein (ORL) (Bunzow et al., 1994; Chen et al., 1994; Fukuda et al., 1994; Mollereau et al., 1994; Nishi et al., 1994; Wang et al., 1994; Wick et al., 1994; Lachowicz et al., 1995). Despite its structural resemblance to opioid peptides, nociceptin/orphanin FQ (N/OFQ) selectively binds to the ORL receptor but not to μ-, δ-, and κ-opioid receptor subtypes, whereas opioid peptides were found to exert no action on the ORL receptor (Mollereau et al., 1994; Lachowicz et al., 1995; Reinscheid et al., 1995). At the cellular level, the actions of N/OFQ appear similar to those of opioid peptides (Standifer and Pasternak, 1997). The ORL receptor is coupled to G-proteins (Meunier et al., 1995; Reinscheid et al., 1995), whose activation resulted in inhibition of adenylyl cyclase activity (Meunier et al., 1995; Reinscheid et al., 1995), modulation of calcium (Knoflach et al., 1996) and potassium conductances (Connor et al., 1996a; Vaughan and Christie, 1996; Ikeda et al., 1997; Vaughan et al., 1997), and regulation of transmitter release (Liebel et al., 1997; Neal et al., 1997; Vaughan et al., 1997). At the behavioral level, systemic application of N/OFQ elicited a unique range of responses, including pronociceptive (Meunier et al., 1995; Reinscheid et al., 1995) or antinociceptive (Xu et al., 1996; Erb et al., 1997; King et al., 1997; Yamamoto et al., 1997) effects, and impairment of or increases in locomotion (Reinscheid et al., 1995; Florin et al., 1996), depending on the concentration that was administered. A more general role of N/OFQ seems to be related to blockade of stress and reversal of opioid-mediated antinociception (Mogil et al., 1996). A recent study demonstrated N/OFQ anxiolytic-like effects in mice and rats that were consistent across several behavioral paradigms generating different types of fear-like responses by exposure to various stressful environmental conditions (Jenck et al., 1997).

One important central structure involved in the integration of fear and anxiety is the amygdala (Davis, 1992; LeDoux, 1995; Maren and Fanselow, 1996). In addition, amygdaloid mechanisms have been shown to be involved in analgesic processes (Helmstetter et al., 1995; Manning and Mayer, 1995; Pavlovic et al., 1996). ORL receptors, N/OFQ and its precursor protein, are expressed in relatively high densities in the various subnuclei of the amygdala, as has been demonstrated through *in situ* hybridization and immunohistochemical and autoradiographic procedures (Bunzow et al., 1994; Mollereau et al., 1994; Wick et al., 1994; Lachowicz et al., 1995; Anton et al., 1996; Nothacker et al., 1996; Schulz et al., 1996; Florin et al., 1997). In addition, autoradiographic studies showed a particularly strong effect of N/OFQ-mediated receptor-activation of G-proteins in the amygdaloid complex (Shimohira et al., 1997; Sim and Childers, 1997).

Although results from behavioral and histochemical studies thus suggest a role of N/OFQ within the integrative function of the amygdala, more direct evidence supporting this hypothesis is missing. The present study was therefore undertaken to investigate in detail the effects of N/OFQ in the amygdala on the cellular level, using electrophysiological and pharmacological techniques in the slice preparation of the rat amygdala *in vitro*. The experiments were focused on the lateral (AL) and central (ACe) nuclei, which represent the main input and output structures of the amygdala, respectively (Pitkänen et al., 1997).

MATERIALS AND METHODS

Preparation. Long–Evans rats of either sex [postnatal days (P) 11–16] were anesthetized with halothane and killed by decapitation. A block of tissue containing the amygdala was rapidly removed and placed in

Received June 29, 1998; revised July 30, 1998; accepted July 30, 1998.

This work was supported by the Kultusministerium des Landes Sachsen-Anhalt (FKZ 2279A/0085H) and the Deutsche Forschungsgemeinschaft (SFB 426, TP B3). We thank Professor V. Höllt for stimulating the work on N/OFQ, and A. Ritter, R. Ziegler, and A. Reupsch for expert technical assistance.

Correspondence should be addressed to Hans-Christian Pape, Institut für Physiologie, Medizinische Fakultät, Otto-von-Guericke-Universität, Leipziger Strasse 44, D-39120 Magdeburg, Germany.

ice-cold oxygenated physiological saline containing (in mM): KCl 2.4, $MgSO_4$ 10, $CaCl_2$ 0.5, piperazine-*N,N′*-bis(ethanesulfonic acid) (PIPES) 20, glucose 10, sucrose 195, pH 7.35. Coronal slices (300 μm thick) were prepared on a Vibratome (Model 1000, Ted Pella, Redding, CA) and incubated in standard artificial CSF (ACSF) of the following composition (in mM): NaCl 120, KCl 2.5, NaH_2PO_4 1.25, $NaHCO_3$ 22, $MgSO_4$ 2, $CaCl_2$ 2, glucose 20, bubbled with 95%O_2/5% CO_2 to pH 7.3. Slices were kept at 34°C for 20 min and for up to 8 hr at 24–25°C. A single slice was transferred to the recording chamber and submerged in ACSF, at a perfusion rate of ~2 ml/min. The tissue was fixed by a silk mesh around a horseshoe-shaped platinum wire.

Recording techniques. Neurons located superficially at a depth of ~50 μm on the dorsal surface of the slice were approached under visual control by differential interference contrast (Axioskop FS, Achroplan 40/w; Zeiss, Oberkochen, Germany) infrared videomicroscopy (S/W-camera CF8/1, Kappa, Gleichen, Germany) (Dodt and Zieglgänsberger, 1994). Electrophysiological recordings were performed using the patch-clamp technique in whole-cell mode (Hamill et al., 1981) with a patch-clamp amplifier (EPC-7, List Medical Systems, Darmstadt, Germany). Patch pipettes were pulled from borosilicate glass (GC150TF-10, Clark Electromedical Instruments, Pangbourne, UK). After the whole-cell configuration was obtained, cells were held at −70 mV unless indicated otherwise. In each slice, only one neuron was recorded. Drugs were added to the external ACSF. In some experiments, the extracellular KCl concentration was elevated to 5, 7.5, or 10 mM by substitution of an equimolar amount of NaCl. In 0 Ca^{2+} solution, $CaCl_2$ was replaced by $MgCl_2$. Pipettes were filled with (in mM): potassium gluconate 95, K_3 citrate 20, NaCl 10, HEPES 10, $MgCl_2$ 1, $CaCl_2$ 0.1, BAPTA 1, MgATP 3, NaGTP 0.5, pH 7.2 with KOH. In some experiments, 2 mM GDP-β-S or 100 μM GTP-γ-S were included in the internal solution in exchange for NaGTP. Typical electrode resistances were 2.5–3 MΩ in the bath, with access resistances in the range of 5 to 7 MΩ. Errors attributable to series resistance were <2.5 mV. A liquid junction potential of 10 mV was corrected (Neher, 1992). Records were low-pass-filtered at 2.5 kHz (eight-pole Bessel filter). Voltage-clamp experiments were performed using pClamp software operating via a Labmaster DMA interface (Axon Instruments, Foster City, CA) on a PC. Experiments were conducted at 24–25°C. All substances were obtained from Sigma (Diesenhofen, Germany), except for nociceptin/orphanin FQ and [$Phe^1\psi(CH_2$-$NH)Gly^2$]NC(1–13)NH_2, which were purchased from Gramsch Laboratories (München, Germany) and Tocris (Langford, UK), respectively. Data are presented as mean ± SEM.

Histological procedures. In some experiments, 0.1% biocytin was added to the intracellular solution. After recordings, slices containing a biocytin-filled cell were immersed in 4% paraformaldehyde in PBS (in mM: NaCl 120, NaH_2PO_4 10, K_2HPO_4 30, thimerosal 0.05, pH 7.4 with NaOH) for 48 hr and then cryoprotected in a solution composed of 30% sucrose in PBS for 24 hr. Slices were then sectioned at a thickness of 100 μm using a freezing microtome (Leica, Benzheim, Germany) and rinsed three times (5 min each) with PBS. Endogenous peroxidase reaction was by-passed by incubation in 0.3% H_2O_2 in PBS for 30 min. Sections were then treated with the avidin–biotin complex horseradish peroxidase (PK 4000, 1:100; Vector Laboratories, Burlingame, CA) in PBS supplemented with 0.03% Triton X-100 and 2% bovine serum albumin overnight. Between steps, sections were rinsed three times for 15 min each with PBS. The immunohistochemical reaction was completed by adding 3,3′diaminobenzidine (0.5 mg/ml) and H_2O_2 (0.01%) to the incubation medium, including 0.02% $(NH_4)_2Ni(SO_4)_2 \times 6\ H_2O$ and 0.025% $CoCl_2$, and stopped after 6 min by rinsing with PBS (two times for 5 min). Sections were mounted on chromalaun gelatin-coated coverslips, dehydrated, and coverslipped in DePeX (Serva Feinbiochemica, Heidelberg, Germany) mounting media.

Pertussis toxin treatment. Slices were rinsed three times with sterile medium of the following composition: 200 ml Eagle's basal medium, 100 ml HBSS, 100 ml inactivated horse serum (all from Life Technologies, Eggenstein, Germany), 2 mM glutamine, and 0.65% glucose, pH 7.3. The tissue was then affixed to coverslips with a chicken plasma (Cocalico, Reamstown, PA) clot coaggulated by thrombin (25 U/ml; Calbiochem, Bad Soden, Germany) and cultured in a roller incubator (Heraeus, Hanau, Germany) for ~18 hr at 34°C. Slices were kept in medium supplemented with 500 ng/ml pertussis toxin, and control slices were incubated in medium with no added pertussis toxin. Control and treated slices were used for recording alternately to confirm the viability of the neurons.

RESULTS

Recordings were derived from a total of 94 neurons in the AL and 55 cells in the ACe. Lateral amygdaloid neurons typically possessed a pyramidal-like cell body with spiny dendrites, as revealed by intracellular staining with biocytin (Fig. 1*A*) ($n = 14$). Central amygdaloid neurons had a heterogeneous morphological appearance with piriform to ovoid cell bodies and mostly spiny dendrites (Fig. 1*B*) ($n = 11$).

Application of N/OFQ (1 μM) through bath perfusion resulted in a transient outward current associated with an increase in membrane conductance (Fig. 1*C*) in 92 of 94 recorded AL neurons. The average maximal amplitude of the outward current deflection induced by 1 μM N/OFQ at a holding potential of −70 mV was 53.3 ± 7.3 pA ($n = 8$). Similar responses to N/OFQ were observed during blockade of synaptic transmission in the presence of 1.5 μM TTX (61.1 ± 7.0 pA; $n = 4$) or in Ca^{2+}-free solution (55.9 ± 20.3 pA; $n = 3$), indicating a direct postsynaptic response of the recorded neurons (data not shown).

Increase in K^+ conductance through N/OFQ in AL neurons

Hyperpolarizing voltage steps of 350 msec duration applied between −80 and −140 mV in 10 mV increments elicited slowly developing currents in AL neurons (Fig. 2*A*). Application of N/OFQ (1 μM) increased these membrane currents. The effect of N/OFQ was isolated by subtracting currents obtained before and during action of the peptide. The difference currents showed rapid activation and no inactivation during the 350 msec voltage pulse. Ramp–voltage commands (0.2 mV/msec) applied from −70 to −140 mV revealed a membrane current with inwardly rectifying properties that was increased by 1 μM N/OFQ (Fig. 2*B*). Current–voltage (*I–V*) relationships (Fig. 2*C,D*) obtained by plotting the N/OFQ-induced current amplitude at the end of the hyperpolarizing step against voltage (Fig. 2*C*) or by the ramp protocol (Fig. 2*D*) were similar in that they demonstrated moderate inward rectification. The N/OFQ-induced current reversed at approximately −100 mV, i.e., very close to the K^+ equilibrium potential as calculated by the Nernst equation ($E_K = -104.1$ mV). To confirm the contribution of K^+ as the main charge carrier of the N/OFQ-induced membrane current, the K^+ concentration of the perfusing saline was varied (Fig. 3). Ramp–voltage commands were applied at 0.07 Hz to monitor the *I–V* relationship during the experiment. The reversal potential of the N/OFQ-evoked response induced by a 10-fold change in the external K^+ concentration had a slope of 53.7 mV, i.e., similar to that predicted by the Nernst equation for a pure K^+ electrode (Fig. 3*B*). Furthermore, increases in the extracellular K^+ concentration were associated with an increase in the slope of the *I–V* relationship. Such behavior is typical of inward rectifiers (Fig. 3*A*) (Isomoto et al., 1997).

Pharmacological properties of the N/OFQ response

To obtain full recovery of N/OFQ responses during pharmacological experiments, the concentration of the peptide was reduced to 50 nM. Because the response on the first application of N/OFQ was often larger in amplitude compared with those to further applications, presumably because of desensitization phenomena (Ikeda et al., 1997), the order of application of N/OFQ alone and N/OFQ in the presence of antagonists was varied in different cells. In a first series of experiments, possible effects of N/OFQ on opioid receptors were tested through the use of the nonselective opioid receptor antagonist naloxone (Fig. 4*A*) (Raynor et al.,

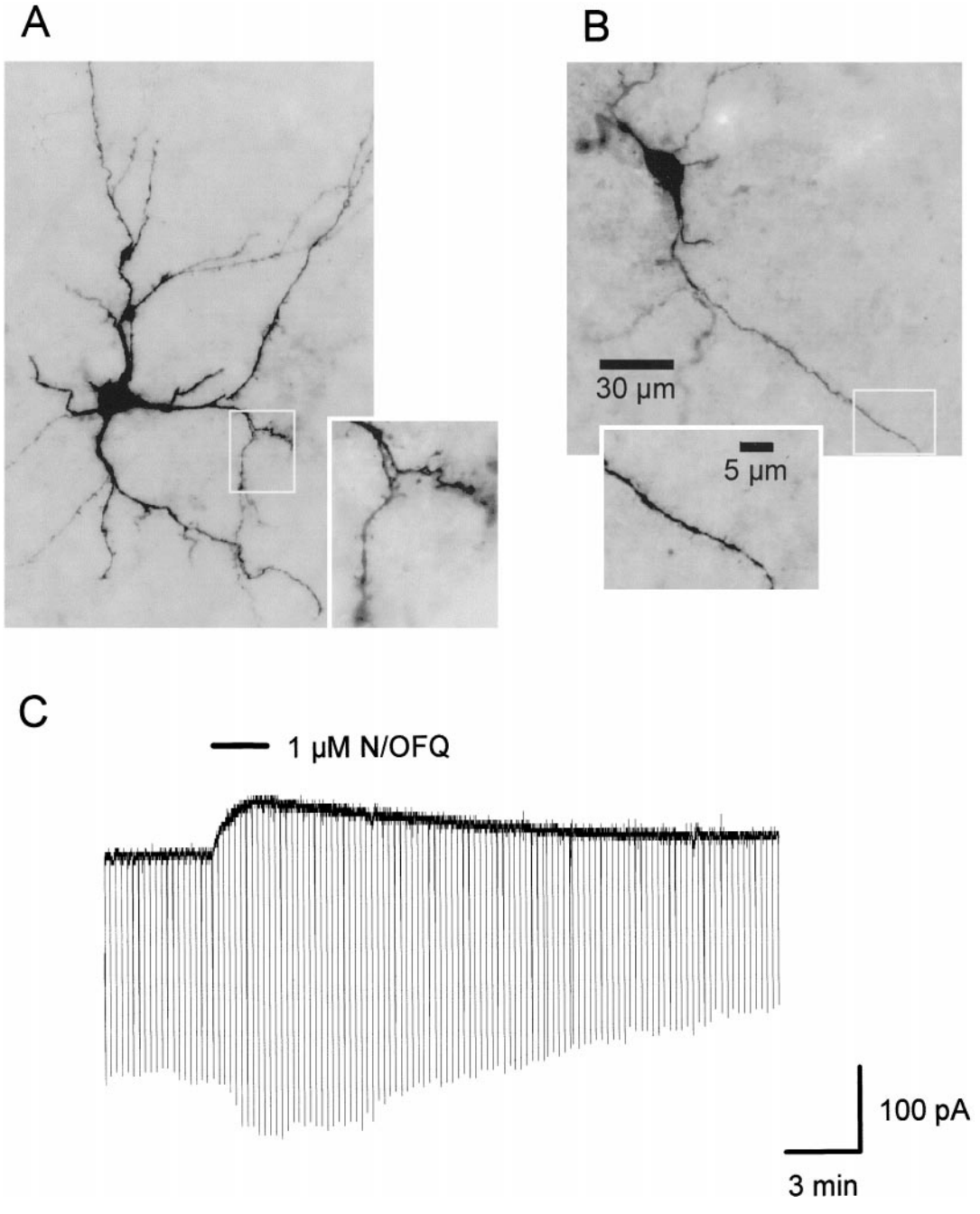

Figure 1. Typical morphology of neurons recorded in the lateral (*A*) and central (*B*) amygdaloid nucleus. *Insets* illustrate that dendrites were covered with numerous spines. Scale bars in *B* also apply to *A*. *C*, Typical response of an amygdaloid neuron to N/OFQ. Under voltage-clamp conditions, application of N/OFQ (as indicated above current trace) evokes a transient outward current from a holding potential of −70 mV. Downward deflections represent current responses to ramp–voltage commands from −70 to −140 mV (0.2 mV/msec) that were applied at 0.07 Hz to monitor the membrane input conductance. Note that the N/OFQ-induced current is associated with an increase in input conductance.

1994). N/OFQ elicited an outward current of 43.0 ± 3.7 pA (n = 5), which was not altered by the addition of 10 μM naloxone (44.8 ± 6.6 pA; n = 5). By comparison, the selective antagonist to the ORL receptor [Phe$^1\psi$(CH$_2$-NH)Gly^2]NC(1–13)NH$_2$ (Guerrini et al., 1998) reduced the response to 50 nM N/OFQ in a concentration-dependent manner (Fig. 4*B*). The antagonistic effect was quantified as reduction in the maximal N/OFQ-induced current amplitude during the presence of [Phe$^1\psi$(CH$_2$-NH)Gly^2]NC(1–13)NH$_2$ compared with the control N/OFQ response in an individual cell. Half-maximal inhibition was obtained at 760 nM [Phe$^1\psi$(CH$_2$-NH)Gly^2]NC(1–13)NH$_2$ with a Hill coefficient of 0.89 (n = 31) (Fig. 4*B*).

The effect of N/OFQ was substantially and reversibly reduced through application of 100 μM Ba^{2+} (Fig. 4*C*). The effect of Ba^{2+} on N/OFQ responses could not be analyzed in an individual cell, because applications of N/OFQ for periods longer than 3 min led to a current that did not return to baseline during the typical recording time of 60–80 min. This may be attributable to slow dissociation of the ligand (Ardati et al., 1997) and/or slow washout of the drug during bath perfusion (Muller et al., 1988). On

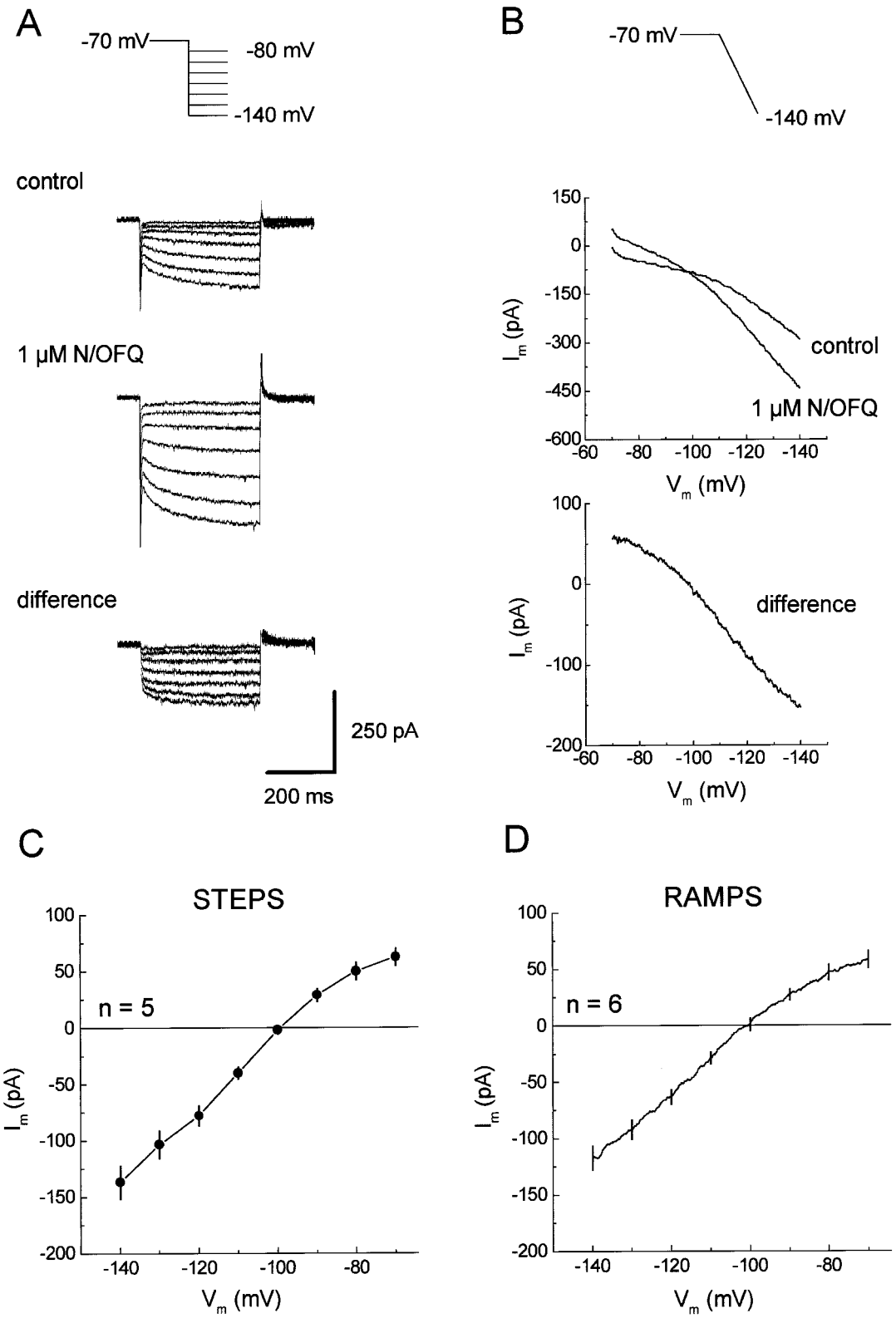

Figure 2. Activation of an inwardly rectifying membrane conductance through N/OFQ. All recordings were obtained from neurons in the AL before (*control*) and during application of 1 μM N/OFQ. *A*, Families of inward currents evoked by hyperpolarizing voltage steps in the range of −80 to −140 mV for 350 msec (holding potential −70 mV). The difference obtained from recordings before and during action of N/OFQ represents the N/OFQ-induced currents. Note the time-dependent inward rectification of the currents. *B*, *I–V* relationships obtained from voltage ramps (0.2 mV/msec) between −70 and −140 mV. The difference conductance (subtraction of *I–V* relationships during action of N/OFQ from controls) displays inward rectification. *C, D*, Average *I–V* relationships derived by plotting the N/OFQ-induced steady-state current amplitude against voltage (*C*, $n = 5$; voltage steps as in *A*) or by using the ramp protocol (*D*, $n = 6$; protocol as in *B*). Currents reverse near −100 mV, i.e., close to the presumed K^+ equilibrium potential, and display inward rectification.

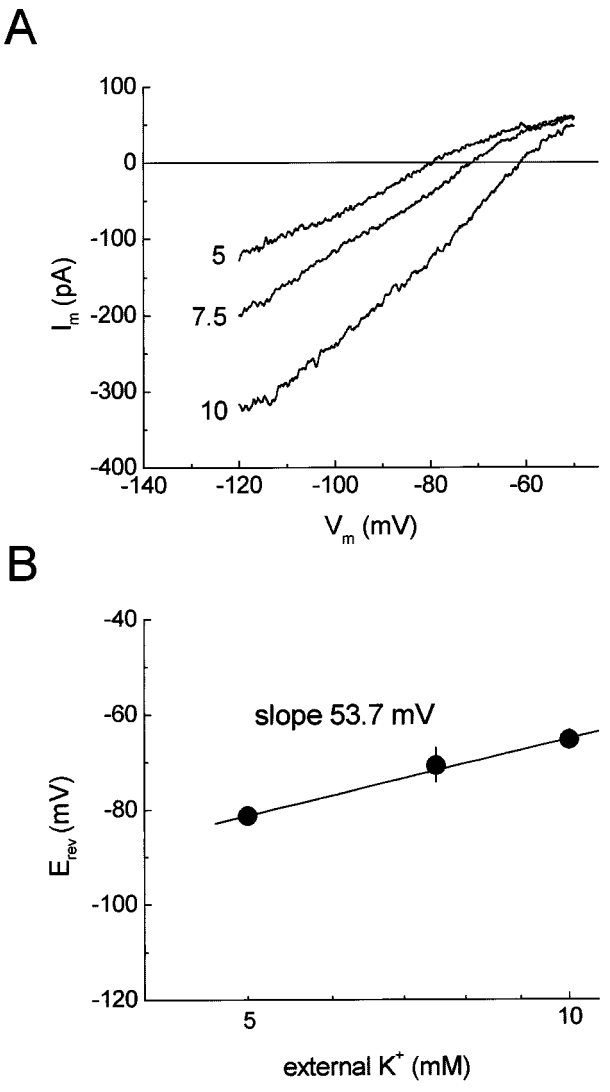

Figure 3. K^+ dependence of N/OFQ-evoked currents in AL neurons. *A*, *I–V* relationships of the N/OFQ-sensitive current monitored by ramp protocols (0.2 mV/msec, 0.07 Hz) at various external K^+ concentrations (as indicated in mM near traces). *B*, Shift of reversal potentials of the N/OFQ-evoked current at various external K^+ concentrations according to the Nernst equation with a slope of 53.7 mV. Data represent averages and SEM obtained from three different cells at each concentration using ramp protocols as in *A*. The line was fitted by linear regression.

average, Ba^{2+} blocked 39.3 ± 6.6 pA (n = 6) of the N/OFQ-sensitive current, corresponding to a reduction of the maximal amplitude by 87.4 ±. 6.6% (n = 6).

Concentration–response relationship of the N/OFQ response

Concentration–response relationships of N/OFQ were investigated in an elevated extracellular K^+ concentration (10 mM) at a holding potential of −80 mV, to increase the driving force and hence the magnitude of the N/OFQ-induced current. In an individual neuron, only one N/OFQ concentration was tested, and concentration–response relationships were constructed from maximal responses to a given concentration. The N/OFQ-induced current showed clear concentration-dependency (Fig. 5). The half-maximal effect (EC_{50}) was elicited by 30.6 nM with a Hill coefficient of 0.63 (n = 36).

Involvement of G-proteins

Next, the possible mediation by G-proteins of the N/OFQ-induced K^+ current was tested (Fig. 6). The tip of the electrode was filled with standard pipette solution, and the remainder was backfilled with a solution supplemented with 100 μM GTP-γ-S, a nonhydrolyzable GTP analog (Gilman, 1987). Under these conditions, N/OFQ (50 nM) evoked an outward current shortly after establishing the whole-cell configuration, with no indication of recovery during the time course of the experiment (Fig. 6*A*, compare with Fig. 4*A*). A second application of N/OFQ had no further effect, whereas the standing current was significantly reduced by Ba^{2+} (Fig. 6*A*) (n = 3). Inclusion in the pipette solution of 2 mM GDP-β-S, a nonhydrolyzable GDP analog (Gilman, 1987), resulted in only a small outward current (9.4 ± 1.3 pA) in response to a first application of N/OFQ, whereas further applications failed to evoke an effect (Fig. 6*B*) (n = 3). Finally, after incubation of slices in a medium containing pertussis toxin (500 ng/ml) for ~18 hr at 34°C, N/OFQ effects could not be obtained in any neuron tested (Fig. 6*C*) (n = 3). In slices that had been similarly treated, but with no addition of the toxin, all cells tested responded to N/OFQ (1 μM) with the typical outward current (maximal amplitude at a holding potential of −70 mV; 30.3 ± 4.2 pA; n = 4).

N/OFQ responses in central amygdaloid neurons

In 17 of 55 neurons recorded in the ACe, N/OFQ (1 μM) elicited a current with properties similar to that in AL cells, in that it possessed inwardly rectifying properties (Fig. 7*A*), it was reduced to 74.2 ± 5.4% by 100 μM Ba^{2+} (n = 7) (Fig. 7*B*), and its reversal potential shifted in a Nernstian manner with the external K^+ concentration (Fig. 7*E*). The maximal current amplitude at a holding potential of −70 mV was significantly ($p < 0.01$) smaller in neurons of the ACe (21.6 ± 4.1 pA; n = 9) compared with that in the AL (53.3 ± 7.3 pA; n = 8). In 24 central amygdaloid neurons, no responses to N/OFQ were detected (data not shown). The remainder of the cells recorded in the ACe responded to N/OFQ with a small current (8.6 ± 1.1 pA at a holding potential of −70 mV; n = 14) (Fig. 7*D*), which displayed no inward rectification as measured by the ramp protocol (Fig. 7*C*) but was also blocked by 100 μM Ba^{2+} (Fig. 7*D*).

Effect of N/OFQ on spike firing

Under current-clamp conditions, 50 nM N/OFQ induced a membrane hyperpolarization from the resting membrane potential of −70 mV, with an average maximal amplitude of 10.3 ± 1.2 mV in AL neurons (n = 7) (Fig. 8*A*). The input membrane resistance decreased from 535.7 ± 58.3 to 326.4 ± 30.3 MΩ during the maximal response (n = 7). This hyperpolarization and decrease in input resistance had a dampening effect on cell excitability, as was indicated by a substantial reduction in the number of spikes evoked by depolarizing current responses before and during action of N/OFQ (Fig. 8*B*).

DISCUSSION

The results of the present study indicate that N/OFQ acts on ORL receptors in the postsynaptic membrane of neurons in the rat lateral and central amygdaloid nuclei, thereby inducing an increase in an inwardly rectifying K^+ conductance mediated via pertussis toxin-sensitive G-proteins. This promotes significant hyperpolarization of the resting membrane potential, an increase in input conductance, and a decrease in cellular excitability. Responses to N/OFQ were quantitatively different in various

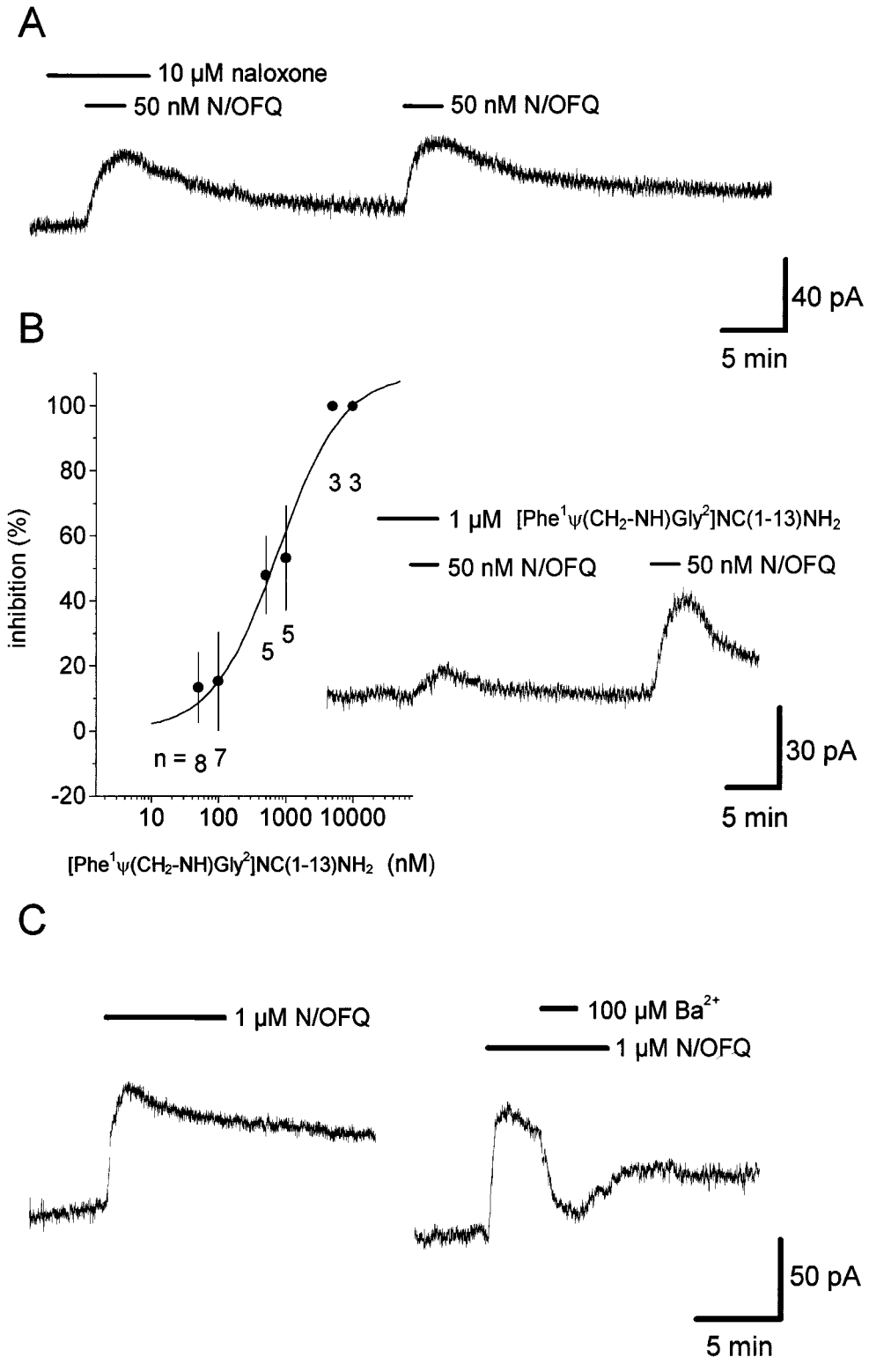

Figure 4. Pharmacological properties of the N/OFQ-sensitive current. Responses were obtained in AL neurons at a holding potential of −70 mV. Substance application as indicated above current traces. *A*, Similar responsiveness to N/OFQ (50 nM) in a given cell with and without presence of naloxone (10 μM). *B*, Substantial reduction of N/OFQ (50 nM) responses during presence of the ORL selective antagonist [Phe$^1\psi$(CH$_2$-NH)Gly^2]NC(1–13)NH$_2$. Diagram represents the concentration–response relationship of the antagonist (see Results for further details). The number of cells tested for each concentration is indicated near error bars. The curve was drawn according to the equation $I = I_{max}/\{1 + (EC_{50}/A)^n\}$, where I represents the current response, I_{max} the maximal current amplitude, A the concentration of the agonist N/OFQ, and n the Hill coefficient. The EC_{50} and Hill values obtained from the curve were 762.8 nM and 0.89, respectively. *C*, Sensitivity of the N/OFQ-induced current to external Ba^{2+}. During prolonged application of N/OFQ (1 μM), the induced current slowly declines and persists after cessation of drug application. In a different cell, addition of 100 μM Ba^{2+} for 2 min reversibly reduces the N/OFQ (1 μM)-sensitive current.

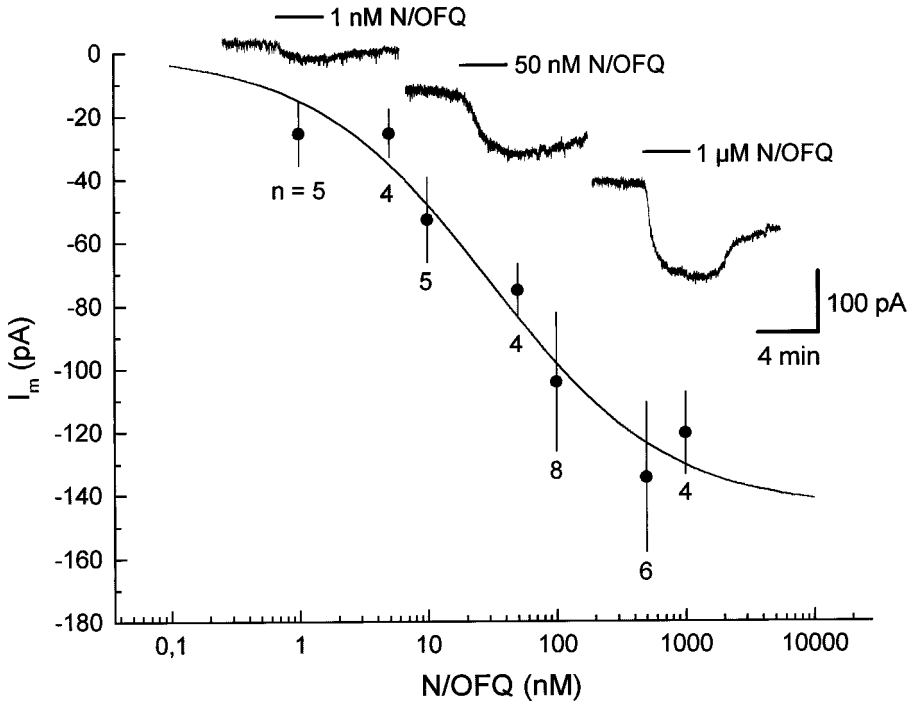

Figure 5. Concentration–response relationship of the N/OFQ-induced current in AL neurons. Experiments were conducted in 10 mM external K^+ concentration with a holding potential of −80 mV, resulting in inward currents in response to N/OFQ application. Examples for membrane currents examined in the presence of 1 μM, 50 nM, and 1 nM N/OFQ are presented as *insets*. Data are averages from measurements in different numbers of cells, as indicated near error bars. In a given neuron, only one N/OFQ concentration was tested. The curve was drawn according to the Hill equation (as in Fig. 4). The EC_{50} and Hill values obtained from the curve were 30.6 nM and 0.63, respectively.

subnuclei of the amygdala, in that almost every presumed projection class I neuron encountered in the AL was responsive, whereas a typical response was obtained in roughly one-third of neurons in the ACe.

Mediation of N/OFQ responses through ORL receptors

The involvement of ORL receptors is indicated by three lines of evidence. First, responses to N/OFQ were reversibly blocked by the selective ORL receptor antagonist [Phe$^1\psi$(CH$_2$-NH)Gly^2]NC(1–13)NH$_2$ (Guerrini et al., 1998), whereas naloxone, a prototypical antagonist to the μ-, δ-, and κ-subtypes of opioid receptors (Raynor et al., 1994), was ineffective even at high concentrations. In the guinea-pig ileum and in mouse vas deferens, 1 μM [Phe$^1\psi$(CH$_2$-NH)Gly^2]NC(1–13)NH$_2$ reportedly reduced the effect of 50 nM N/OFQ by ~80%, compared with a 61% reduction of N/OFQ-induced response in amygdaloid neurons. These results support the idea of a selective effect of N/OFQ on ORL receptors in the present study. Second, the concentration–response relationships of N/OFQ found in amygdaloid neurons (EC_{50} = 30.6 nM) are comparable to those reported earlier for various types of cellular responses to N/OFQ, including increases in K^+ conductance (EC_{50} between 12 and 90 nM) (Connor et al., 1996a; Vaughan and Christie, 1996; Ikeda et al., 1997; Vaughan et al., 1997; Wagner et al., 1998), reduction of calcium currents (EC_{50} at 42–80 nM) (Connor et al., 1996b; Knoflach et al., 1996), and inhibition of K^+-evoked glutamate release (EC_{50} = 51 nM) (Nicol et al., 1996). Third, mRNA-expressing ORL receptors and ORL receptor binding sites were demonstrated to be highly enriched in the amygdala (Bunzow et al., 1994; Mollereau et al., 1994; Wick et al., 1994; Lachowicz et al., 1995; Anton et al., 1996; Florin et al., 1997). In addition, the mRNA of the N/OFQ precursor protein (Houtani et al., 1996; Nothacker et al., 1996) and immunoreactivity against the peptide (Schulz et al., 1996) were detected in this limbic area. Therefore, it seems reasonable to assume a functional role of the ORL receptor/N/OFQ peptide system in the amygdala.

Involvement of G-protein-coupled K^+ channels

The primary structure of ORL displays the seven putative membrane-spanning domains of a G-protein-coupled membrane receptor (Bunzow et al., 1994; Fukuda et al., 1994; Mollereau et al., 1994; Wick et al., 1994; Lachowicz et al., 1995). Indeed, N/OFQ potently inhibited forskolin-stimulated cAMP accumulation in transfected cells (Meunier et al., 1995; Reinscheid et al., 1995) and modulated Ca^{2+} conductances via pertussis toxin-sensitive G-proteins in acutely isolated hippocampal neurons (Knoflach et al., 1996) and SH-SY5Y neuroblastoma cells (Connor et al., 1996b). By comparison, the inhibition of the T-type Ca^{2+} channel in rat sensory neurons induced by N/OFQ occurred through a G-protein-independent mechanism (Abdulla and Smith, 1997).

Three lines of evidence suggest that in amygdaloid neurons, the activation of ORL through N/OFQ resulting in an increase in an inward rectifier K^+ conductance appears to be mediated by a G-protein-linked pathway. First, during the intracellular presence of GTP-γ-S, a nonhydrolyzable GTP analog (Gilman, 1987), N/OFQ evoked sustained responses, presumably attributable to irreversible activation of the G-proteins. Second, intracellular GDP-β-S, the nonhydrolyzable GDP analog (Gilman, 1987), significantly reduced the response amplitude to a first application of N/OFQ and prevented further responses in individual cells, presumably caused by functional inactivation of the G-proteins. Third, incubation of slices overnight with pertussis toxin, a blocker of the G_i/G_0 class of G-proteins (Hille, 1994), prevented responses to N/OFQ, whereas slices that were similarly treated, but with no addition of the toxin, showed qualitatively unaltered responsiveness to N/OFQ. Taken together, these data indicated a coupling of ORL to the G_i/G_0 class of G-proteins (Hille, 1994).

In amygdaloid neurons, the targets of ORL activation appear to be the inwardly rectifying types of K^+ channels (Fakler and Ruppersberg, 1996; Isomoto et al., 1997; Karschin et al., 1997), as was indicated by the *I–V* relationship of responses to N/OFQ and

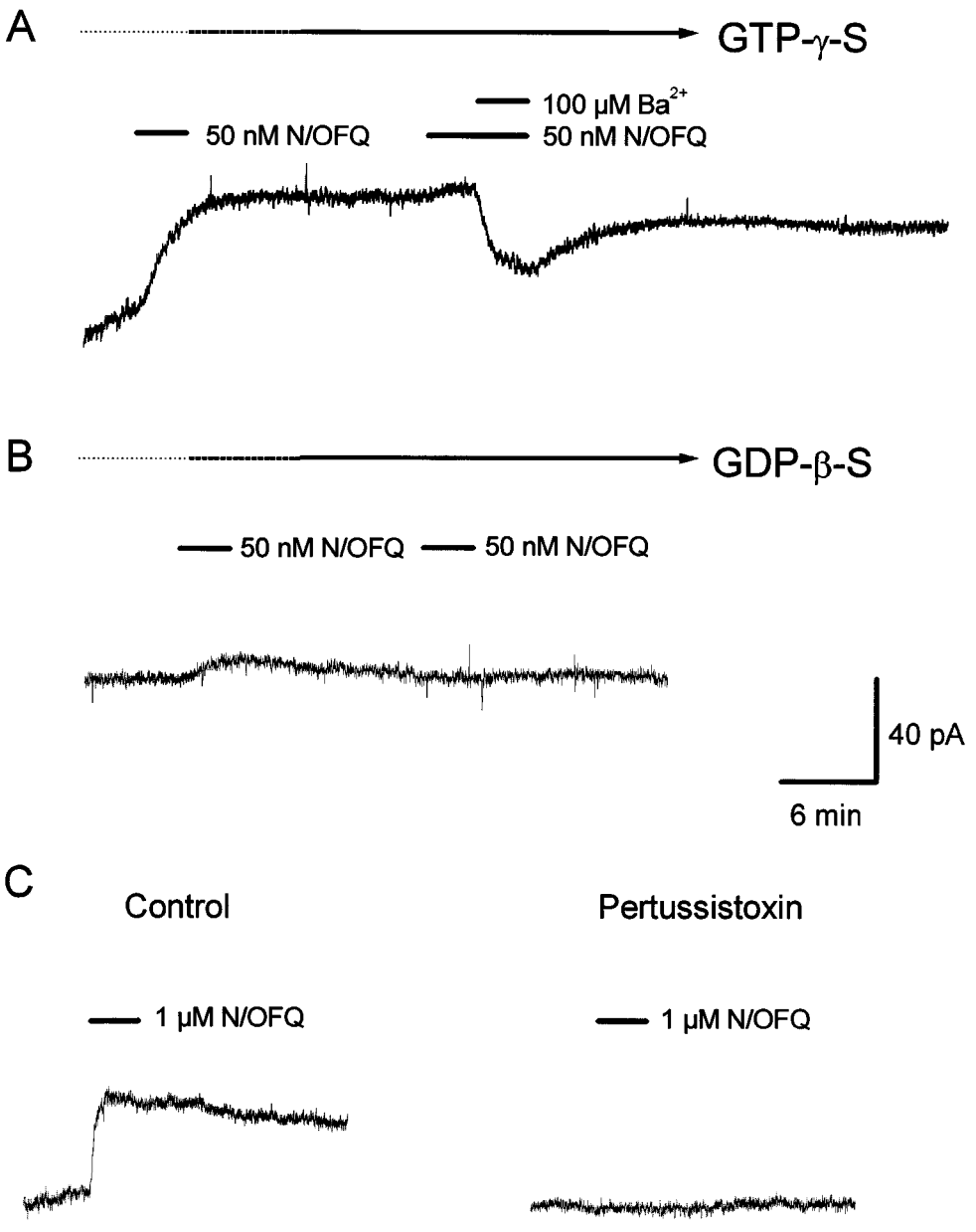

Figure 6. Mediation via G-proteins of the N/OFQ-sensitive current in AL neurons. *A*, Inclusion of GTP-γ-S (100 μM) in the recording pipette results in a sustained outward current in response to a single application of 50 nM N/OFQ. A second application of N/OFQ has no further effect, whereas the induced current is still sensitive to Ba^{2+} (100 μM). *B*, With GDP-β-S (2 mM) in the pipette, N/OFQ elicits a small outward current, which cannot be repeated on subsequent application. *C*, After incubation of the slices in a medium containing pertussis toxin (500 ng/ml), application of N/OFQ has no effect, whereas cells in slices that had been incubated with no toxin added (*Control*) showed typical responses to N/OFQ.

their sensitivity to low concentrations of extracellular Ba^{2+}. This hypothesis is supported by results from *in situ* hybridization studies showing that the mRNA of subunits of G-protein-coupled K^+ channels, namely Kir3.1, Kir3.2, Kir3.3, are expressed in high density in amygdaloid nuclei (Karschin et al., 1996). By comparison, only low levels of mRNA of "classical" inwardly rectifying K^+ channels belonging to the Kir2 family are present in the amygdala (Karschin et al., 1996). The inwardly rectifying properties of membrane currents observed under control conditions (Fig. 2*A,B*) may thus represent the background conductance of G-protein-gated channels (Dascal, 1997) or an H-current component rather than classical inward rectifier activity (Womble and Moises, 1993). The exact subunit composition of the G-protein-gated inward rectifier channels mediating responses to N/OFQ remains to be elucidated, although the fast but not instantaneous activation of the N/OFQ-induced current (Fig. 2*A*) suggests an involvement of Kir3.1 subunits.

N/OFQ and "classical" opioid effects in the amygdala

At the cellular level, N/OFQ and opioid peptides seem to share a number of common mechanisms, such as the increase in a G-protein-coupled inwardly rectifying K^+ conductance, whereas on the systemic level, N/OFQ can potently reverse opioid analgesia (Darland et al., 1998). In the AL, an opioid-induced hyperpolarization presumably mediated through an increase in K^+ conductance reportedly occurs in the nonpyramidal type of cells (type 2), whereas cells similar in appearance to those termed class I by McDonald (1992) were nonresponsive (Sugita and North, 1993). AL neurons that were labeled with biocytin in the present study possessed morphologies indicative of class I neurons, suggesting that the effects of N/OFQ and opioids are mediated by different subsets of neurons. The observation that only a comparatively small percentage of the morphologically heterogeneous group of neurons encountered in the ACe was responsive to N/OFQ seems to be supportive of this hypothesis. A more direct

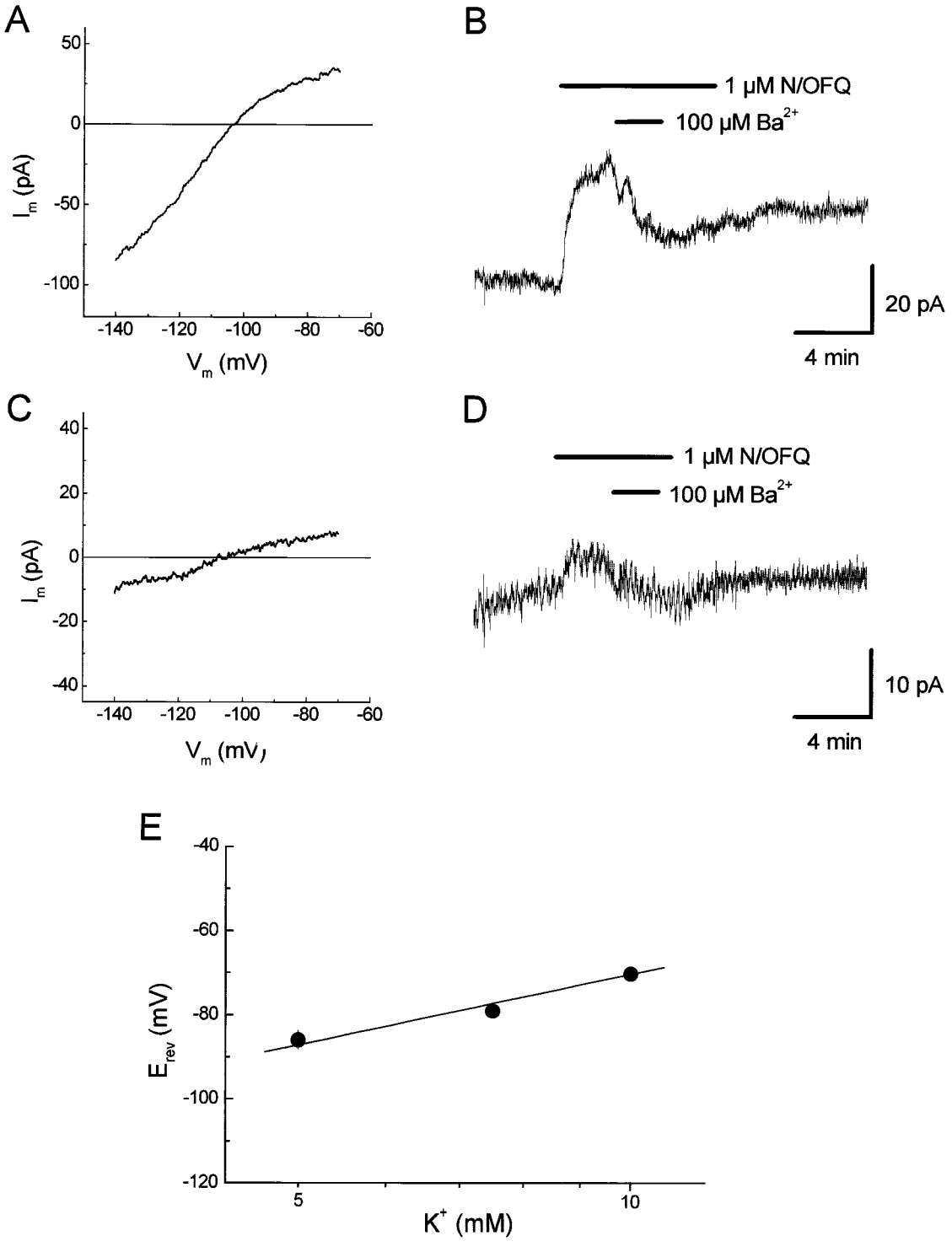

Figure 7. N/OFQ responsiveness in ACe neurons. In two different cells, N/OFQ elicits an inwardly rectifying current (*A*, ramp protocol as in Fig. 2) and a small current with no apparent rectification (*C*). The N/OFQ-evoked currents are sensitive to external Ba^{2+} (100 μM) in both cells (*B, D*). *E*, Reversal potentials of the N/OFQ-induced currents shift on variation of the external K^+ concentration with a slope of 55.8 mV according to the Nernst equation (*E*). For each K^+ concentration, four cells were tested.

correlation between morphologically defined types of cells and N/OFQ responsiveness will require immunocytochemical analyses of the cellular distribution of receptors and K^+ channels in identified types of cells in the various parts of the amygdala.

Possible source and functional significance of N/OFQ

The expression of N/OFQ mRNA, ORL mRNA, and the ORL protein, as determined through *in situ* hybridization and immunocytochemical techniques, is very dense to dense in the amyg-

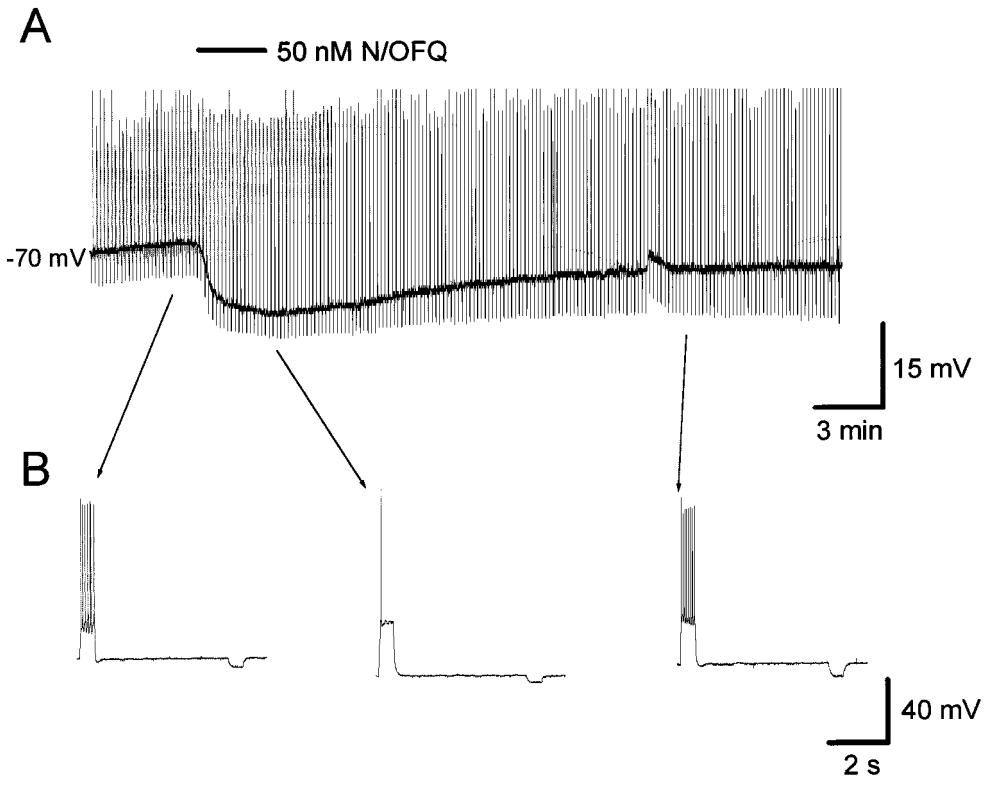

Figure 8. Reduced excitability of an AL neuron during action of N/OFQ recorded under current-clamp conditions. *A*, Application of 50 nM N/OFQ induces a transient hyperpolarizing response from a membrane potential close to the resting value (−70 mV) associated with a decrease in apparent input resistance (as indicated by responses to small hyperpolarizing test pulses). Examples in *B* illustrate responses to depolarizing test pulses (+150 pA, 500 msec, 0.1 Hz) and hyperpolarizing test pulses (−20 pA) at a faster time scale at times indicated. Note the reduction in spike activity during action of N/OFQ. Spikes are truncated. Resting membrane potential was −67.7 mV.

dala (Bunzow et al., 1994; Mollereau et al., 1994; Anton et al., 1996; Houtani et al., 1996; Nothacker et al., 1996; for review, see Henderson and McKnight, 1997; Meunier, 1997; Darland et al., 1998). Although these data suggest that N/OFQ may act as a transmitter of the abundant interneurons inherent to the amygdaloid complex (Nitecka and Frotscher, 1989; Smith and Paré, 1994), electrical stimulation at different sites within the amygdala or the external capsule using different stimulus protocols failed to evoke a postsynaptic potential sensitive to the selective ORL antagonist in the present study (data not shown). On the other hand, a dense expression of N/OFQ or its receptor, or both, has been found to exist in various regions with axonal projection to the amygdala, including the ventral tegmental area, the locus coeruleus, and the dorsal raphe nuclei of the brain stem (LeDoux, 1995; LeDoux and Muller, 1997), which may as well give rise to an N/OFQ-releasing system. Further analyses, such as an electron microscopic study, will be needed for the detection of N/OFQ at the synaptic level and thus the identification of the substrates of N/OFQ-mediated neurotransmission in the amygdala.

In any case, ~98 and 55% of the cells encountered in the AL and ACe, respectively, responded to local application of N/OFQ. Morphological identification of the N/OFQ-sensitive neurons with intracellular injection of biocytin revealed characteristics indicative of projection cells (McDonald, 1992, 1996), such as pyramidal-shaped spiny cells in the AL and morphologically more heterogeneous types of cells in the ACe, all of which possessed spine-rich dendrites. Following from this is the conclusion that synaptic transmission mediated through N/OFQ is not negligible in the amygdala. The hyperpolarizing effect and associated decrease in excitability produced by N/OFQ, in turn, indicates that N/OFQ promotes a net dampening effect on amygdaloid output activity. In view of the known role of the amygdala for the integration of sensory and aversive signals (Davis, 1992; LeDoux, 1995; Maren and Fanselow, 1996), with the lateral and central nucleus serving as the main input and output station, respectively (Pitkänen et al., 1997), these conclusions support the speculation that the N/OFQ-induced dampening of amygdaloid output activity contributes to the reduction in fear responsiveness that has been observed recently during systemic application of this neuropeptide in mice and rats (Jenck et al., 1997). Studies should now be performed that combine local application of the selective ORL antagonist $[Phe^1\psi(CH_2\text{-}NH)Gly^2]NC(1\text{–}13)NH_2$ in the amygdala, with behavioral paradigms generating various types of fear responses, to understand the exact conditions under which N/OFQ is acting as an anxiolytic.

REFERENCES

Abdulla FA, Smith PA (1997) Nociceptin inhibits T-type Ca^{2+} channel current in rat sensory neurons by a G-protein-independent mechanism. J Neurosci 17:8721–8728.

Anton B, Fein J, To T, Li X, Silberstein L, Evans CJ (1996) Immunohistochemical localization of ORL-1 in the central nervous system of the rat. J Comp Neurol 368:229–251.

Ardati A, Henningsen RA, Higelin J, Reinscheid RK, Civelli O, Monsma FJ (1997) Interaction of [^{3}H] orphanin FQ and ^{125}I-Tyr14-orphanin FQ with the orphanin FQ receptor: kinetics and modulation by cations and guanine nucleotides. Mol Pharmacol 51:816–824.

Bunzow JR, Saez C, Mortrud M, Bouvier C, Williams JT, Low M, Grandy DK (1994) Molecular cloning and tissue distribution of a putative member of the rat opioid receptor gene family that is not a μ, δ, or κ opioid receptor type. FEBS Lett 347:284–288.

Chen Y, Fan Y, Liu J, Mestek A, Tian M, Kozak CA, Yu L (1994) Molecular cloning, tissue distribution and chromosomal localization of a novel member of the opioid receptor gene family. FEBS Lett 347:279–283.

Connor M, Vaughan CW, Chieng B, McDonald JC (1996a) Nociceptin receptor coupling to a potassium conductance in rat locus coeruleus neurones *in vitro*. Br J Pharmacol 119:1614–1618.

Connor M, Yeo A, Henderson G (1996b) The effect of nociceptin on

Ca^{2+} channel current and intracellular Ca^{2+} in the SH-SY5Y human neuroblastoma cell line. Br J Pharmacol 118:205–207.

Darland T, Heinricher MM, Grandy DK (1998) Orphanin FQ/nociceptin: a role in pain and analgesia, but so much more. Trends Neurosci 21:215–221.

Dascal N (1997) Signalling via the G protein-activated K^+ channels. Cell Signal 9:551–573.

Davis M (1992) The role of the amygdala in fear-potentiated startle: implications for animal models of anxiety. Trends Pharmacol Sci 13:35–41.

Dodt HU, Zieglgänsberger W (1994) Infrared videomicroscopy: a new look at neuronal structure and function. Trends Neurosci 17:453–458.

Erb K, Liebel JT, Tegeder I, Zeilhofer HU, Brune K, Geisslinger G (1997) Spinally delivered nociceptin/orphanin FQ reduces flinching behaviour in the rat formalin test. NeuroReport 8:1967–1970.

Fakler B, Ruppersberg JP (1996) Functional and molecular diversity classifies the family of inward-rectifier K^+ channels. Cell Physiol Biochem 6:195–209.

Florin S, Suaudeau C, Meunier J-C, Costentin J (1996) Nociceptin stimulates locomotion and exploratory behaviour in mice. Eur J Pharmacol 317:9–13.

Florin S, Leroux-Nicollet I, Meunier J-C, Costentin J (1997) Autoradiographic localization of [^{3}H]nociceptin binding sites from telencephalic to mesencephalic regions of the mouse brain. Neurosci Lett 230:33–36.

Fukuda K, Kato S, Mori K, Nishi M, Takeshima H, Iwabe N, Miyata T, Houtani T, Sugimoto T (1994) cDNA cloning and regional distribution of a novel member of the opioid receptor family. FEBS Lett 343:42–46.

Gilman AG (1987) G proteins: transducers of receptor-generated signals. Annu Rev Biochem 56:615–649.

Guerrini R, Calo G, Rizzi A, Bigoni R, Bianchi C, Salvadori S, Regoli D (1998) A new selective antagonist of the nociceptin receptor. Br J Pharmacol 123:163–165.

Hamill OP, Marty A, Neher E, Sakmann B, Sigworth FJ (1981) Improved patch-clamp techniques for high-resolution current recording from cells and cell-free membrane patches. Pflügers Arch 391:85–100.

Helmstetter FJ, Bellgowan PSF, Poore LH (1995) Microinfusion of *mu* but not *delta* or *kappa* opioid agonists into the basolateral amygdala results in inhibition of the tail flick reflex in pentobarbital-anesthetized rats. J Pharmacol Exp Ther 275:381–388.

Henderson G, McKnight AT (1997) The orphan opioid receptor and its endogenous ligand: nociceptin/orphanin FQ. Trends Pharmacol Sci 18:293–301.

Hille B (1994) Modulation of ion-channel function by G protein-coupled receptors. Trends Neurosci 17:531–536.

Houtani T, Nishi M, Takeshima H, Nukada T, Sugimoto T (1996) Structure and regional distribution of nociceptin/orphanin FQ precursor. Biochem Biophys Res Commun 219:714–719.

Ikeda K, Kobayashi K, Kobayashi T, Ichikawa T, Kumanishi T, Kishida H, Yano R, Manabe T (1997) Functional coupling of the nociceptin/orphanin FQ receptor with the G-protein-activated K^+ (GIRK) channel. Mol Brain Res 45:117–126.

Isomoto S, Kondo C, Kurachi Y (1997) Inwardly rectifying potassium channels: their molecular heterogeneity and function. Jpn J Physiol 47:11–39.

Jenck F, Moreau J-L, Martin JR, Kilpatrick GJ, Reinscheid RK, Monsma FJ, Nothacker H-P, Civelli O (1997) Orphanin FQ acts as an anxiolytic to attenuate behavioral responses to stress. Proc Natl Acad Sci USA 94:14854–14858.

Karschin C, Diβmann E, Stühmer W, Karschin A (1996) IRK(1–3) and GIRK(1–4) inwardly rectifying K^+ channel mRNAs are differentially expressed in the adult rat brain. J Neurosci 16:3559–3570.

Karschin A, Wischmeyer E, Döring F, Karschin C (1997) Inwardly rectifying Kir channels: primitive channel structures as basis for functional diversity. Neuroforum 3:127–132.

King MA, Rossi GC, Chang AH, Williams L, Pasternak GW (1997) Spinal analgesic activity of orphanin FQ/nociceptin and its fragments. Neurosci Lett 223:113–116.

Knoflach F, Reinscheid RK, Civelli O, Kemp JA (1996) Modulation of voltage-gated calcium channels by orphanin FQ in freshly dissociated hippocampal neurons. J Neurosci 16:6657–6664.

Lachowicz JE, Shen Y, Monsma FJ, Sibley DR (1995) Molecular cloning of a novel G protein-coupled receptor related to the opiate receptor family. J Neurochem 64:34–40.

LeDoux JE (1995) Emotion: clues from the brain. Annu Rev Psychol 46:209–235.

LeDoux JE, Muller J (1997) Emotional memory and psychopathology. Philos Trans R Soc Lond B Biol Sci 352:1719–1726.

Liebel JT, Swandulla D, Zeilhofer HU (1997) Modulation of excitatory synaptic transmission by nociceptin in superficial dorsal horn neurones of the neonatal rat spinal cord. Br J Pharmacol 121:425–432.

Manning BH, Mayer DJ (1995) The central nucleus of the amygdala contributes to the production of morphine antinociception in the rat tail-flick test. J Neurosci 15:8199–8213.

Maren S, Fanselow MS (1996) The amygdala and fear conditioning: has the nut been cracked? Neuron 16:237–240.

McDonald AJ (1992) Cell types and intrinsic connections of the amygdala. In: The amygdala: neurobiological aspects of emotion, memory, and mental dysfunction (Aggleton JP, ed), pp 67–96. New York: Wiley-Liss.

McDonald AJ (1996) Glutamate and aspartate immunoreactive neurons of the rat basolateral amygdala: colocalization of excitatory amino acids and projections to the limbic circuit. J Comp Neurol 365:367–379.

Meunier J-C (1997) Nociceptin/orphanin FQ and the opioid receptor-like ORL1 receptor. Eur J Pharmacol 340:1–15.

Meunier J-C, Mollereau C, Toll L, Suaudeau C, Moisand C, Alvinerie P, Butour J-L, Guillemot J-C, Ferrara P, Monsarrat B, Mazarguil H, Vassart G, Parmentier M, Costentin J (1995) Isolation and structure of the endogenous agonist of opioid receptor-like ORL_1 receptor. Nature 377:532–535.

Mogil J S, Grisel JE, Reinscheid RK, Civelli O, Belknap JK, Grandy DK (1996) Orphanin is a functional anti-opioid peptide. Neuroscience 75:333–337.

Mollereau C, Parmentier M, Mailleux P, Butour J-L, Moisand C, Chalon P, Caput D, Vassart G, Meunier J-C (1994) ORL1, a novel member of the opioid receptor family: cloning, functional expression and localization. FEBS Lett 341:33–38.

Muller W, Misgeld U, Heinemann U (1988) Carbachol effects on hippocampal neurons *in vitro*: dependence on the rate of rise of carbachol tissue concentration. Exp Brain Res 72:287–298.

Neal MJ, Cunningham JR, Paterson SJ, McKnight AT (1997) Inhibition by nociceptin of the light-evoked release of Ach from retinal cholinergic neurones. Br J Pharmacol 120:1399–1400.

Neher E (1992) Correction for liquid junction potentials in patch clamp experiments. Methods Enzymol 207:123–131.

Nicol B, Lambert DG, Rowbotham DJ, Smart D, McKnight AT (1996) Nociceptin induced inhibition of K^+ evoked glutamate release from rat cerebrocortical slices. Br J Pharmacol 119:1081–1083.

Nishi M, Takeshima H, Mori M, Nakagawara K, Takeuchi T (1994) Structure and chromosomal mapping of genes for the mouse kappa-opioid receptor and an opioid receptor homologue (MOR-C). Biochem Biophys Res Commun 205:1353–1357.

Nitecka L, Frotscher M (1989) Organization and synaptic interconnections of GABAergic and cholinergic elements in the rat amygdaloid nuclei: single- and double-immunolabeling studies. J Comp Neurol 279:470–488.

Nothacker H-P, Reinscheid RK, Mansour A, Henningsen RA, Ardati A, Monsma FJ, Watson SJ, Civelli O (1996) Primary structure and tissue distribution of the orphanin FQ precursor. Proc Natl Acad Sci USA 93:8677–8682.

Pavlovic ZW, Cooper ML, Bodnar RJ (1996) Opioid antagonists in the periaqueductal gray inhibit morphine and β-endorphin analgesia elicited from the amygdala of rats. Brain Res 741:13–26.

Pitkänen A, Savander V, LeDoux JE (1997) Organization of intra-amygdaloid circuitries in the rat: an emerging framework for understanding functions of the amygdala. Trends Neurosci 20:517–523.

Raynor K, Kong H, Chen Y, Yasuda K, Yu L, Bell GI, Reisine T (1994) Pharmacological characterization of the cloned κ-, δ-, and μ-opioid receptors. Mol Pharmacol 45:330–334.

Reinscheid RK, Nothacker H-P, Bourson A, Ardati A, Henningsen RA, Bunzow JR, Grandy DK, Langen H, Monsma FJ, Civelli O (1995) Orphanin FQ: a neuropeptide that activates an opioidlike G protein-coupled receptor. Science 270:792–794.

Schulz S, Schreff M, Nüβ D, Gramsch C, Höllt V (1996) Nociceptin/orphanin FQ and opioid peptides show overlapping distribution but not co-localization in pain-modulatory brain regions. NeuroReport 7:3021–3025.

Shimohira I, Tokuyama S, Himeno A, Niwa M, Ueda H (1997) Characterization of nociceptin-stimulated in situ [^{35}S]GTPγS binding in com-

parison with opioid agonist-stimulated ones in brain regions of the mice. Neurosci Lett 237:113–116.

Sim LJ, Childers SR (1997) Anatomical distribution of mu, delta, and kappa opioid- and nociceptin/orphanin FQ-stimulated [^{35}S]guanylyl-5′-*O*-(γ-thio)-triphosphate binding in guinea pig brain. J Comp Neurol 386:562–572.

Smith Y, Paré D (1994) Intra-amygdaloid projections of the lateral nucleus in the cat: PHA-L anterograde labeling combined with postembedding GABA and glutamate immunocytochemistry. J Comp Neurol 342:232–248.

Standifer KM, Pasternak GW (1997) G proteins and opioid receptor-mediated signalling. Cell Signal 9:237–248.

Sugita S, North RA (1993) Opioid actions on neurons of rat lateral amygdala in vitro. Brain Res 612:151–155.

Vaughan CW, Christie MJ (1996) Increase by the ORL_1 receptor (opioid receptor-like$_1$) ligand, nociceptin, of inwardly rectifying K conductance in dorsal raphe nucleus neurones. Br J Pharmacol 117:1609–1611.

Vaughan CW, Ingram SL, Christie MJ (1997) Actions of the ORL_1 receptor ligand nociceptin on membrane properties of rat periaqueductal gray neurons *in vitro*. J Neurosci 17:996–1003.

Wagner EJ, Rønnekleiv OK, Grandy DK, Kelly MJ (1998) The peptide orphanin FQ inhibits β-endorphin neurons and neurosecretory cells in the hypothalamic arcuate nucleus by activating an inwardly-rectifying K^+ conductance. Neuroendocrinology 67:73–82.

Wang JB, Johnson PS, Imai Y, Persico AM, Ozenberger BA, Eppler CM, Uhl G R (1994) cDNA cloning of an orphan opiate receptor gene family member and its splice variant. FEBS Lett 348:75–79.

Wick MJ, Minnerath SR, Lin X, Elde R, Law P-Y, Loh HH (1994) Isolation of a novel cDNA encoding a putative membrane receptor with high homology to the cloned μ, δ, and κ opioid receptors. Mol Brain Res 27:37–44.

Womble MD, Moises HC (1993) Hyperpolarization-activated currents in neurons of the rat basolateral amygdala. J Neurophysiol 70:2056–2065.

Xu X-J, Hao J-X, Wiesenfeld-Hallin Z (1996) Nociceptin or antinociceptin: potent spinal antinociceptive effect of orphaninFQ/nociceptin in the rat. NeuroReport 7:2092–2094.

Yamamoto T, Nozaki-Taguchi N, Kimura S (1997) Analgesic effect of intrathecally administered nociceptin, an opioid receptor-like$_1$ receptor agonist, in the rat formalin test. Neuroscience 81:249–254.